Lightweight Signal Processing Algorithms for Human Activity Monitoring using Dual PIR-sensor Nodes

Muhammad Tahir*, Peter Hung*, Ronan Farrell*, Seán Mcloone* and Tim McCarthy†
*Institute of Microelectronics and Wireless Systems
†National Centre for Geocomputation
National University of Ireland Maynooth, Maynooth, Co. Kildare, Ireland
Email: {mtahir, phung, rfarrell, sean.mcloone}@eeng.nuim.ie, tim.mccarthy@nuim.ie

***Abstract*—A dual Pyroelectric InfraRed (PIR) sensor node is used for human activity monitoring by using simple data processing techniques. We first point out the limitations of existing approaches, employing PIR sensors, for activity monitoring. We study the spectral characteristics of the sensor data for the cases of varying distance between the sensor and moving object as well as the speed of the object under observation. The sampled data from two PIR sensors, is first processed individually to determine the activity window size, which is then fed to a simple algorithm to determine direction of motion. We also claim that human count can be obtained for special scenarios. Preliminary results of our experimentation show the effectiveness of the simple algorithm proposed and give us an avenue for estimating more involved parameters used for speed and localization.**

***Index Terms*—Multi-sensor, activity monitoring, data fusion, pyroelectric IR.**

I. Introduction

Human activity monitoring has always been of much importance, because of a large class of applications, ranging from surveillance to tracking and from smart environments to navigation. Traditionally, human activity monitoring is performed using image sensors producing large data volumes resulting in huge data processing overheads. This may be required to extract certain features of interest, for instance, number of people, position, direction and speed of motion [1] to name a few. Although activity monitoring approaches based on visual sensor solutions provide accurate results, they require large investment and significant infrastructure deployment. Contrary to that, a system based on pyroelectric infrared (PIR) sensors exploit pyroelectricity to detect an object, which is not at thermal equilibrium with its environment [2]. PIR sensors have seen wide deployments in commercial applications, to detect human presence, to trigger security alarms, to control lighting. In addition, these sensors have also found applications in thermal imaging, radiometry, thermometry as well as biometry [3], [4].

While a single PIR sensor is widely used for each surveillance region in security related applications to detect an intruder [5], multiple PIR sensors are needed for more advanced applications such as to achieve coverage [6], assist video surveillance [7] as well as perform tracking [8]. PIR sensors has been used to differentiate a still person from its background [5]. The authors in [6] have employed four PIR sensors to achieve 360° coverage while performing human detection. Since the outputs from all four PIR sensors are fed to the summing amplifier before feeding to the analog-to-digital converter (ADC), this results in inaccessibility of individual sensor outputs to the algorithm. Doing so limits the performance of the sensor node to only human detection. A video surveillance system using multi-modal sensor integration is proposed in [7], where a camera-based tracking system is integrated with a wireless PIR sensor network.

PIR sensors have also been integrated with other sensing modalities to achieve lightweight processing. The problem of localization in a dynamic environment is considered in [9] by using PIR and ultrasonic sensors simultaneously. Linear regression along with smoothing is used for distance correction leading to accurate localization. The multi-modal sensor node design in [6] integrates PIR sensors with acoustic and magnetic sensors to differentiate among humans, soldiers and vehicles. The idea is based on exploiting multiple sensor modalities to achieve the objective.

The task of human monitoring and tracking using PIR sensors can also be implemented in a hierarchical network. This involves the collective actions of sensing modules acting as slaves, a synchronization and error rejection module as a master and a data fusion module termed as a host, as discussed in [8]. In this particular implementation, the geometric sensor module is designed with multiple PIR sensors, each equipped with a Fresnel lens array to obtain a spatially modulated field of view. In addition to tracking, PIR sensors can also be used to detect, differentiate and describe human activity. A multimodal system using a dual PIR sensor node for direction of motion detection using a sensor activation sequence is presented in [7] [10]. The usage of the polarity of the first pulse produced by the sensor for determining the direction of motion limits the applicability of this approach. In [11] the authors have used PIR enabled sensor nodes with information exchange with a base station to determine the direction and number of people. However, this approach is limited due to the requirement for accurate time synchronization across the sensor nodes and

communication overhead involved. Our proposed approach partially addresses these issues by integrating two PIR sensors at each sensor node providing accurate timing for the sampled data from the two PIR sensors and eliminating associated communication overhead.

Rest of the paper is organized as follows. In Section II we discuss the approaches taken in literature to obtain the basic set of parameters, leading to an effective human activity monitoring system. Section III outlines the procedure for data acquisition and the simple algorithms used for processing that data. In Section IV we provide the results for different parameters of interest obtained using simple processing techniques discussed in Section III. Finally, we conclude in Section V with some future directions.

II. Human Activity Monitoring

Usually PIR sensors are designed as part of an overall intrusion detection system, where alarms are activated whenever a PIR output exceeds a predefined threshold. Multiple PIR sensors along with simple signal processing algorithms can be used to obtain parameters of interest for human activity monitoring (e.g. direction of motion, speed and distance of the object and counting these objects to name a few). The first step towards this objective involves distinguishing each individual object and determining its direction of motion as it enters the field-of-view (FOV) of the sensor. The next step involves counting the number of human beings passing through the sensor FOV and estimating the speed of motion. However, there are two key issues in counting the objects, passing by, and measuring their speed of motion.

The first issue is related to counting the number of people passing through the area under observation. There are situations where more than one human being, for instance multiple persons having a conversation and walking parallel to each other are passing through the FOV of the sensor and are close enough to one another that their collective PIR sensor output is almost similar to the case of one person passing. This is because the excitation duration and as a result the size of event window are proportional to human body 'thickness, which appears to be the same for the two scenarios. The second issue is related to speed measurement. Different approaches from the literature, discussed below are limited in their applicability due to the following key features of the sensor response:

- Signal strength at the output of the sensor is not only a function of distance but also speed of the moving object. For instance a relatively slow moving object at the same distance will produce a weaker signal compared to an object moving at a higher speed. This is can be seen from our experimental results shown in Fig. 1. The results in Fig. 1 also show the effect of speed on the spectral characteristics of the output signal.
- The other key aspect of the sensor signal response is the effect of the distance between the sensor and the moving object. The change in distance not only affects the signal strength, but also the spectral characteristics of the sensor response. This can be seen from the experimental results in Fig. 2, where a change in distance from 1 m to 2 m results in a frequency change from 1.2 Hz to 0.55 Hz corresponding to the strongest frequency component.

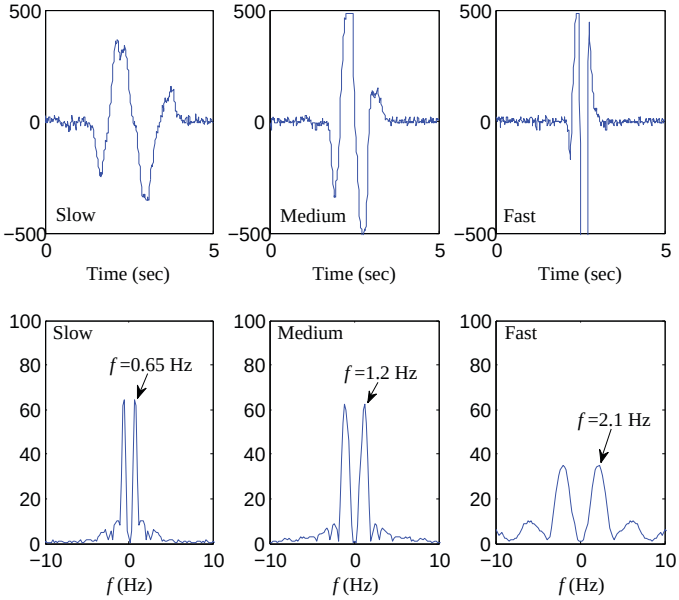

Fig. 1. Experimental results for three different speeds and the corresponding spectrum at a fixed distance form the PIR sensor.

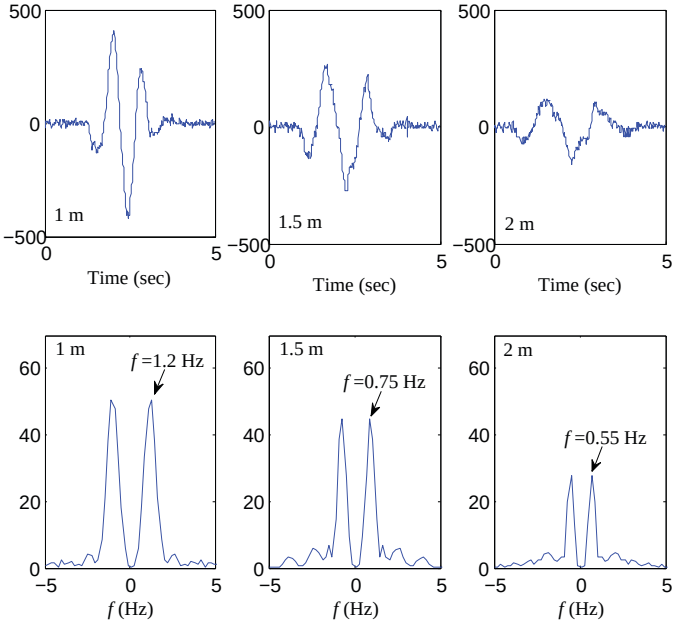

Fig. 2. Spectral characteristics as a function of varying distance between the moving human object and the PIR sensor at a fixed speed.

A. Direction of Motion

A specialized lens arrangement is used in [11] for determining the direction of motion. Specifically, the authors reduced the Fresnel lens horizontal span to a minimum, and choose

a two element PIR sensor, to obtain a phase shift of 180° in the sensor response for the opposite direction. This approach is limited, since using a different lens arrangement or a PIR sensor with an arbitrary number of elements may not give the same response. A multimodal system using a dual PIR sensor node for direction of motion detection using the sensor activation sequence is presented in [7] [10]. Our approach to the problem of direction of motion is somewhat similar to the one in [7], but we measure the phase delay in the responses from the two PIR sensors. The phase delay not only provides an accurate direction detection but also helps in estimating the speed of the moving object.

B. Human Counting

An automated people counting system using low resolution cameras along with a thermal imagery sensor is discussed in [12]. The two imaging systems complement each other in counting people for the low and high density cases. A PIR based direction of motion detection as well as counting of humans, using a specialized Fresnel lens is proposed in [13]. Three physically distributed sensor nodes along the hallway are used for counting people. Two different cases of people walking in line and walking side by side are considered and same direction of motion, for all the objects in the group, is assumed. An accuracy of 75% is claimed for the case when multiple persons are walking side by side.

C. Speed Measurement

The authors in [14] have used the frequency variations as a raw indicator of speed. Twenty repetitive independent back and forth walks are performed for three different speeds namely fast, moderate and slow, along a fixed-path (hence at same distance from the sensor). The authors do not consider the variation in the spectral characteristics as a result of varying the gap between the sensor and the walking person. As we will observe from the empirical results, there is a considerable difference in spectral characteristics due to the varying distance. Hence spectral variations alone can not be used as a measure of speed and it is necessary to take into account the effect of distance.

Another approach used for vehicular traffic speed measurement employing PIR sensors is discussed in [15]. The proposed method is based on measuring the time, the vehicle takes to traverse a fixed distance, between the footprints of the FOVs of the two sensors on the roadway. Consider an object moving at constant speed v and being detected by a PIR sensor for the time interval t. If there are two sensors placed close to each other, such that the midpoints of their FOVs are separated by a distance d, as shown in Fig. 3, then

$$d = \int_{t_1}^{t_2} v dt, \tag{1}$$

where t_1 and t_2 correspond to the time instances when the moving object reaches the sensor FOV midpoints corresponding to the center of the event window. The assumption here is that the object is moving in a narrow pathway (of width c as depicted in Fig. 3) to approximate the distance d as a constant. This results in two sensors producing approximately similar output regardless of how the moving object approaches the detector. For this fixed value of d as depicted in Fig. 3, the expression in (1) can be rewritten as

$$v = \frac{d}{t_2 - t_1} \tag{2}$$

which is used in [14] for speed measurement. The result in (2) can be used to estimate the speed of moving objects only for constant d. This result will not be valid for human activity monitoring, where the distance between the sensor and the moving object changes considerably.

D. Distance Measurement

Distance estimation using two sensor nodes is discussed in [13], where the wireless sensor nodes are installed on the opposite sides of the hallway. They use two different features, the relative amplitude and signal duration from two different sensors, for distance estimation. The results in [13] show that only region based approximate distance classification is possible using this arrangement.

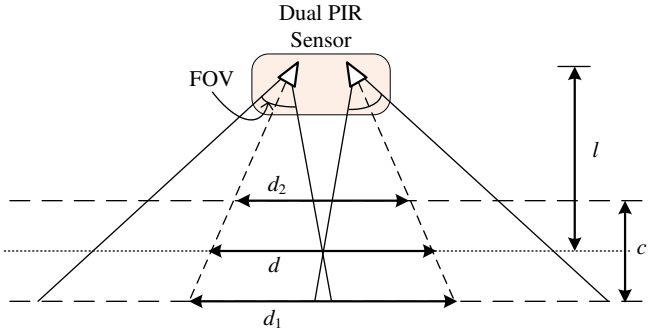

Fig. 3. Physical arrangement of two PIR sensors and their FOV. To limit the error due to relative proximity of the human object to the sensor we assume that $c/l \ll 1$ leading to $d \approx d_1$ and $d \approx d_2$.

III. Data Acquisition and Processing

The data is either sampled directly or amplified before sampling depending on the signal magnitude at the sensor output. Digital potentiometers are used for dynamic amplifier gain control to improve performance range. We have used periodic sampling at a rate of 0.1 kHz for data sampling from two PIR sensors simultaneously. The choice of the sampling rate is to cover a wide range of pedestrian walking speeds. The experiments are performed indoors under bright light conditions.

Data from two PIR sensors mounted on a single node, for distance and speed variation of a single moving object, is analyzed for the spectral characteristics. Zero padding was used to improve the resolution of our small size data set. The frequency components corresponding to peak amplitude at different distances and moving speeds are shown in Fig. 4 and Fig. 5 respectively. As can be seen from the results, an increase

in the distance results in a decrease in the frequency of the strongest spectral component. On the other hand, increasing speed leads to an increase in the frequency as expected.

A. Event Window Calculation

To facilitate human detection and motion tracking, the following data processing is proposed. The duration of each sensor excitation, including the start and end times, should first be found. Then, the number of people as well as their direction of passage through the sensor node viewpoint at a given time interval can be deduced. The RMS values of sensor outputs at event windows are recorded in an attempt to observe its relationship with distance l from the sensor as well as the speed of the moving object. Correlation analysis of delayed sensor outputs is employed to calculate the relative phase delay of both signals, one of the parameters that relates to the speed of object passage.

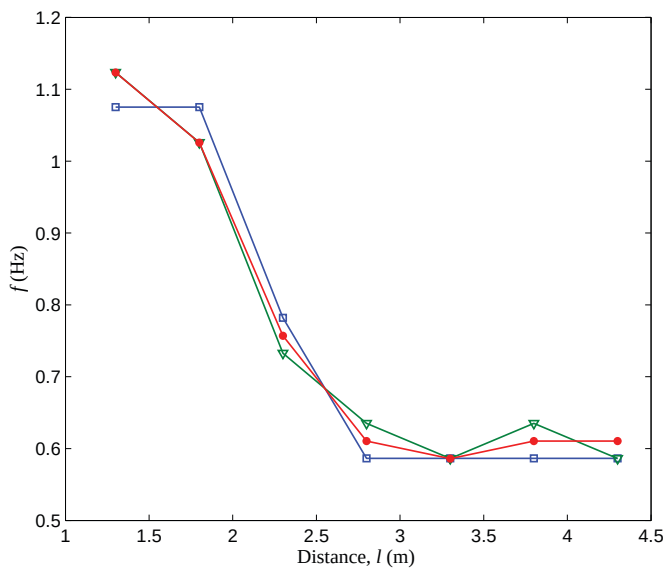

Fig. 4. Spectral characteristics as a function of distance variation between the moving human object and PIR sensor for an approximate fixed speed of 5 km/h.

The general steps used to find the duration of sensor excitation in the form of event window w is illustrated in Fig. 6. As can be seen from Fig. 6, the first low-pass filter is responsible for removing the background noise inherited in the sensor signals and can be different for indoor and outdoor situations. Currently, a third-order Butterworth filter with a cut-off frequency of 5 Hz is employed. The filtered and full-wave rectified signal is then quantized prior to the application to second low-pass filtering. Each individual temporal sensor excitation is segmented by the second first-order Butterworth low-pass filtering with a 0.5 Hz cut-off, which creates an 'enclosure' envelope for each excitation. Finally, a gradient search on the binary signal is performed in each enclosure to detect the event window start and end times, and hence the duration of sensor excitation.

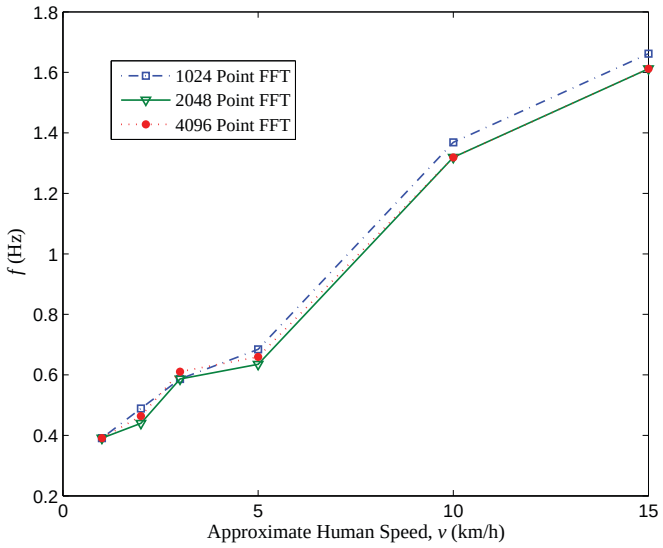

Fig. 5. Variation of spectral characteristics as a function of human speed at a fixed distance of 2.8 m. Experiments for speeds ranging from "slow walking" to "running" are performed.

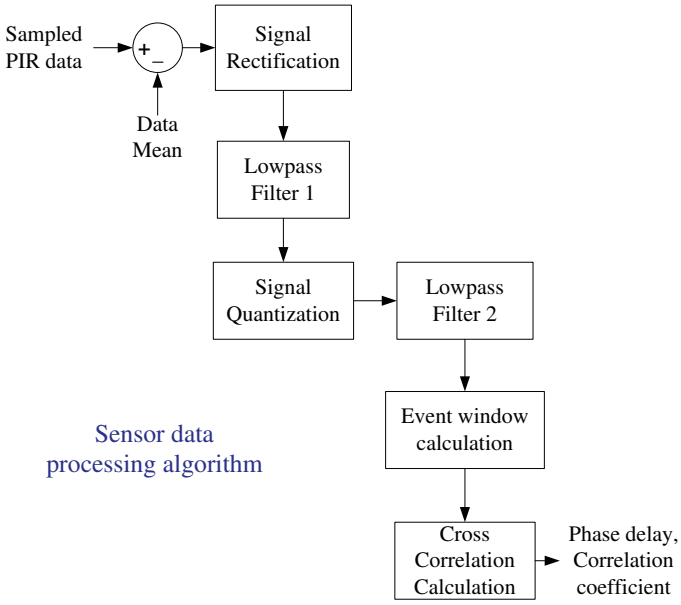

Fig. 6. Block diagram of data processing from single PIR sensor sampled at 10 msec.

During testing, a minimum distance of l (Fig. 3), currently set at 2 m, is used to prevent saturated sensor excitation. Also, it is found that the absolute mean sensor outputs provides more accurate timing information of node excitation compared to zero-mean outputs. This is because a more effective low-pass filtering is possible for non-negative signals compared to the ones with fluctuations above and below the mean value.

B. Human Counting

Due to the incorporation of two PIR sensors in a sensor node, the approaching direction of a human with respect to

the sensor node can readily be checked by comparing the sign of the phase delay between the two sensor outputs. The phase delay can be readily computed as

$$\phi_{delay} = \arg \max_{\phi}[C(y_1(t_{s_1}, t_{e_1}), -y_2(t_{s_2} + \phi, t_{e_2} + \phi))] \quad (3)$$

where ϕ is the relative phase delay in the output from sensor 2 with respect to the sensor 1 output, C denotes the cross-correlation between two signals, $y(a, b)$ represents the sensor output within interval a and b while t_s and t_e are the start and end times of an event window, respectively. Note that the negative polarity in y_2 is to account for the physical arrangement of the two PIR sensors, which are mounted $180°$ phase shifted on the sensor board. Taking this into account would produce a higher average C_{max} than performing cross-correlation analysis for the two sensor outputs with the same polarity. The magnitude of the phase delay is also related to the speed v of human motion, while the magnitude of maximum correlation,

$$C_{max} = C(y_1(t_{s_1}, t_{e_1}), -y_2(t_{s_2} + \phi_{delay}, t_{e_2} + \phi_{delay})) \quad (4)$$

indicates the accuracy of phase delay matching. A value of C_{max} approaching unity suggests near perfect matching. In practice, a maximum absolute phase delay threshold $|\phi_{max}|$ should be included in the data processing to prevent matching with sensor excitations from the previous or the following event windows.

C. Speed and Distance Measurement

Since the speed and distance affect the signal amplitude as well as frequency, it becomes a non-trivial task to measure both parameters simultaneously. One possible approach is to employ multiple sensor nodes and combined their relative position information to estimate these parameters. Alternatively, we can fix one of the parameters to estimate the other, although this leads to a solution with limited practicality. Another possible solution is to consider using multiple sensor modalities to resolve for one parameter. For instance using an ultrasonic sensor we can estimate the distance fairly accurately [9], which can be used to extract the speed from frequency.

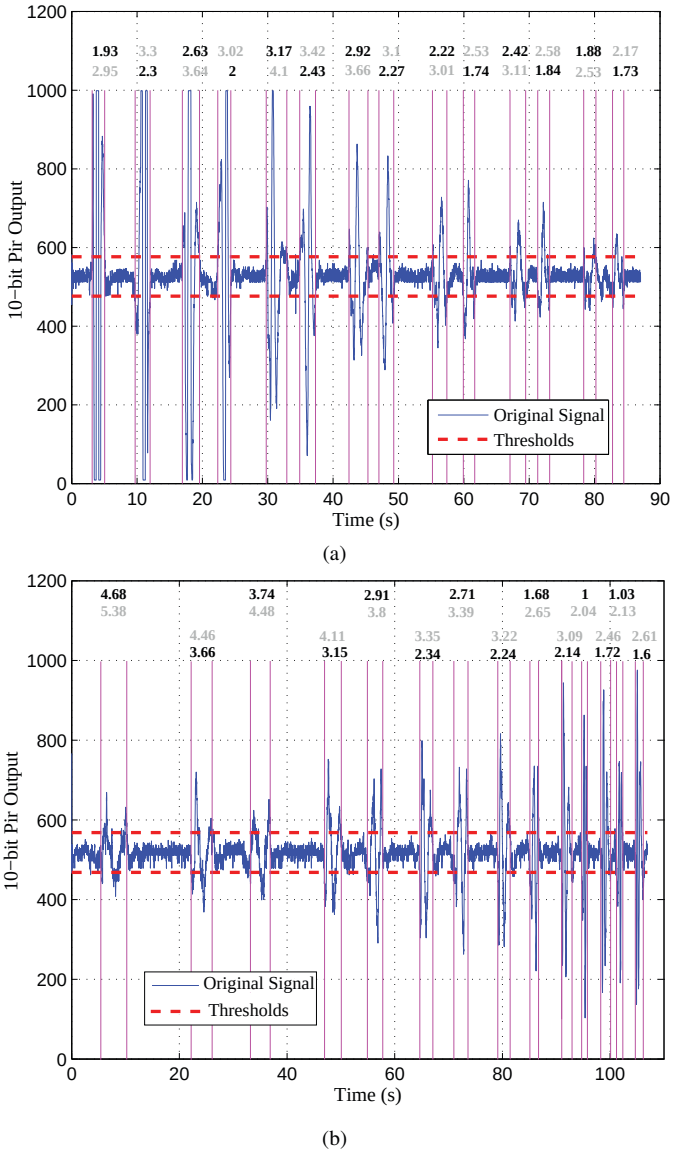

Fig. 7. The raw sensor signal for a moving object and the resulting windowed output for a given threshold level for (a) increasing distance at an approximate speed of 5 km/h, (b) increasing speed at a fixed distance of 2.8 m. The raw signal is obtained from a 10-bit ADC with thresholds at 10 and 1000 to avoid saturation.

IV. Experimental Results

This Section presents some preliminary results on human activity monitoring. Fig. 7(a) shows the raw output of one of the sensors and the event window duration (marked as vertical solid lines with their equivalent numerical values shown in black above the event window) corresponding to the variation in the distance. The numerical values in grey represent the envelop of the filtered signal. The result in Fig. 7(b) shows the results for the variation in speed. As can be observed from Fig. 7(a) that event window duration varies between 3.17s and 1.73s for different distances while for the case of speed variation the event window varies between 4.68s and 1s. By minimizing the event window variation for the case of different distances, it can be used for differentiating the signal spectral changes due to varying speed from those due to varying distance.

The data from two sensors is processed and the maximum cross correlation is computed in order to obtain the phase delay. Table I gives the phase delay corresponding to different distances. Since the person was walking back and forth in front of the two PIR sensors, the resulting phase delay has corresponding sign reversals to show the direction of motion. Table I also gives the cross-correlation coefficients at different distances. This approach for determining the direction of motion is more robust and generalized compared to the polarity based special case. An increase in the phase delay due to increasing distance is because of larger separation between

TABLE I
CROSS-CORRELATION BASED PHASE DELAY VARIATION AS A FUNCTION OF DISTANCE FOR $v = 5$ km/h.

Distance (m)	Phase Delay	Cross-correlation Coefficient
1.3	0.5100	0.7012
1.3	-0.4300	0.8341
1.8	0.7700	0.8980
1.8	-0.6300	0.8694
2.3	0.8300	0.9224
2.3	-0.8300	0.8608
2.8	1.0600	0.8730
2.8	-1.0000	0.6667
3.3	1.1200	0.7927
3.3	-1.0100	0.6537
3.8	1.3600	0.6677
3.8	-1.0900	0.5324

TABLE II
CROSS-CORRELATION BASED PHASE DELAY VARIATION AS A FUNCTION OF SPEED FOR $l = 2.8$ m.

Speed (Kmph)	Phase Delay	Cross-correlation Coefficient
1	2.6900	0.7116
1	-2.0900	0.7878
2	2.0500	0.8217
2	-1.6200	0.7995
3	1.1400	0.8341
3	-1.0800	0.8067
5	1.1000	0.8635
5	-0.9800	0.8171
10	0.6400	0.9130
10	-0.6200	0.8372
15	0.3700	0.8399
15	-0.4200	0.7909

the mid points of the FOVs of the two PIR sensors. The phase delay variation for different speeds and a single object moving back and forth, is provided in Table II. As expected, the phase delay corresponding to higher speed of motion is small, i.e. 0.37 and -0.42 in contrast to the phase delays of 2.69 and -2.09 corresponding to very slow speed.

Using the event window duration and the direction of motion, the objective of counting people can be achieved for the cases: 1) a single person enters or exits at an entrance: 2) multiple people enter or exit in a queue. In the case, where multiple people walking in a queue are close to each other, the sensor excitations do not have any region of inactivity separating the sensor excitations. However, the knowledge of phase delay can be used to get a rough estimate of the speed, which along with event window duration provides the count of the people present in the queue.

We have also studied the effect of distance and speed variations on the received signal strength. Root mean square (RMS) is used as a measure of received signal strength variation. Fig. 8 shows the normalized RMS corresponding to its event window duration as a function of distance. The results show closeness of the RMS values for two opposite directions of motion. The RMS variation as a function of the speed of the moving object is shown in Fig. 9, where the

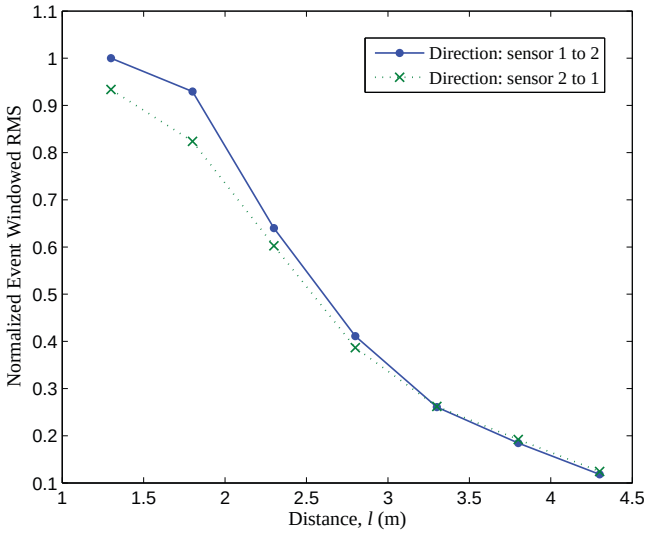

Fig. 8. The Normalized RMS, based on event window duration, as a function of distance variation for $v = 5$ km/h.

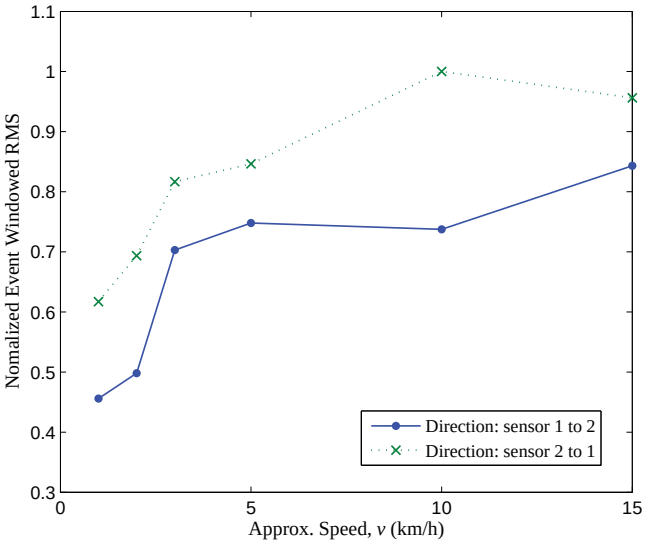

Fig. 9. The Normalized RMS, based on event window duration, as a function of speed variation for $l = 2.8$ m.

responses are different for opposite directions of motion. This is due to the fact that the two sensors had different background views.

To obtain an estimate for the speed a simple algorithm is not possible, because different parameters varying with speed are also affected by distance. For instance, as we observed earlier that the duration of event window changes from 3.17s to 1.73s at different distances for fixed speed v compared to a variation of 4.68s to 1s for the case when the speed is changed for a fixed distance l (Fig. 7). As a result we may not use event window duration for reasonably accurate estimate of distance. This implies that the use of the event window duration along with frequency and amplitude

parameters may not lead to simple algorithms to determine the distance parameter accurately. On the other hand, from Fig. 5, signal frequency changes approximately linearly and is a more reliable parameter for speed estimation by fixing the distance parameter l. Using a curve fit to the speed data in Fig. 5 we obtain the linear relationship of $f = 0.0867v + 0.3$, which can be used to estimate v provided l is fixed. In future we plan to use ultrasonic sensor for estimating the distance along with PIR sensors to develop an improved human activity monitoring system.

V. Discussion and Conclusions

We have developed lightweight signal processing algorithms for sensor nodes equipped with dual Pyroelectric InfraRed (PIR) sensors to achieve the objective of human activity monitoring. First the limitations of the existing approaches for activity monitoring are discussed. Next the spectral characteristics of the sensor data for varying distance and speed of the moving objects are analyzed. Data from dual PIR sensor nodes is first processed individually to determine the activity window size, which is then used to determine direction of motion. Human count for special scenarios can be obtained using the direction of motion and event window durations. Preliminary results of our experimentation show the effectiveness of the simple algorithms proposed. In future, we intend to extend the proposed algorithms for estimating the object speed and localization using distributed algorithms, involving multiple sensor nodes with collaborative sensing, while achieving a real time implementation.

Acknowledgment

Research presented in this paper was funded by a Strategic Research Cluster grant (07/SRC/I1168) by Science Foundation Ireland under the National Development Plan. The authors gratefully acknowledge this support.

References

[1] Q. Cai, J. Aggarwal, R. Inc, and W. Seattle, "Tracking human motion in structured environments using adistributed-camera system," *IEEE Transactions on Pattern Analysis and Machine Intelligence*, vol. 21, no. 11, pp. 1241–1247, 1999.

[2] P. Muralt, "Micromachined infrared detectors based on pyroelectric thin films," *Reports on Progress in Physics*, vol. 64, no. 10, p. 1339, 2001.

[3] C. Tsai and M. Young, "Pyroelectric infrared sensor-based thermometer for monitoring indoor objects," *Review of Scientific Instruments*, vol. 74, p. 5267, 2003.

[4] J. Fang, Q. Hao, D. Brady, M. Shankar, B. Guenther, N. Pitsianis, and K. Hsu, "Path-dependent human identification using a pyroelectric infrared sensor and Fresnel lens arrays," *Optics Express*, vol. 14, no. 2, pp. 609–624, 2006.

[5] D. Karuppiah, P. Deegan, E. Araujo, Y. Yang, G. Holness, Z. Zhu, B. Lerner, R. Grupen, and E. Riseman, "Software mode changes for continuous motion tracking," *Lecture notes in computer science*, pp. 161–180, 2001.

[6] A. Arora, R. Ramnath, E. Ertin, P. Sinha, S. Bapat, V. Naik, V. Kulathumani, H. Zhang, H. Cao, M. Sridharan *et al.*, "Exscal: Elements of an extreme scale wireless sensor network," in *11th IEEE International Conference on Embedded and Real-Time Computing Systems and Applications*, 2005, pp. 102–108.

[7] A. Prati, R. Vezzani, L. Benini, E. Farella, and P. Zappi, "An integrated multi-modal sensor network for video surveillance," in *Proceedings of the third ACM international workshop on Video Surveillance & sensor networks*, 2005, pp. 95–102.

[8] Q. Hao, D. Brady, B. Guenther, J. Burchett, M. Shankar, and S. Feller, "Human tracking with wireless distributed pyroelectric sensors," *IEEE Sensors Journal*, vol. 6, no. 6, pp. 1683–1696, 2006.

[9] D. Kim, J. Choi, M. Lim, and S. Park, "Distance correction system for localization based on linear regression and smoothing in ambient intelligence display," in *Proceedings of Annual International Conference of the IEEE Engineering in Medicine and Biology Society*, 2008, pp. 1443–1446.

[10] R. Cucchiara, A. Prati, R. Vezzani, L. Benini, E. Farella, and P. Zappi, "Using a wireless sensor network to enhance video surveillance," *Journal of Ubiquitous Computing Intelligence*, vol. 1, pp. 1–11, 2006.

[11] P. Zappi, E. Farella, and L. Benini, "Enhancing the spatial resolution of presence detection in a PIR based wireless surveillance network," in *IEEE Conference on Advanced Video and Signal Based Surveillance*, 2007, pp. 295–300.

[12] I. Amin, A. Taylor, F. Junejo, A. Al-Habaibeh, and R. Parkin, "Automated people-counting by using low-resolution infrared and visual cameras," *Measurement*, vol. 41, no. 6, pp. 589–599, 2008.

[13] P. Zappi, E. Farella, and L. Benini, "Pyroelectric InfraRed sensors based distance estimation," in *IEEE Sensors*, 2008, pp. 716–719.

[14] J. Fang, Q. Hao, D. Brady, B. Guenther, and K. Hsu, "A pyroelectric infrared biometric system for real-time walker recognition by use of a maximum likelihood principal components estimation (MLPCE) method," *Optics Express*, vol. 15, no. 6, pp. 3271–3284, 2007.

[15] T. Hussain, A. Baig, T. Saadawi, and S. Ahmed, "Infrared pyroelectric sensor for detection of vehicular traffic using digital signal processing techniques," *IEEE transactions on vehicular technology*, vol. 44, no. 3, pp. 683–689, 1995.